J Inorg Organomet Polym (2015) 25:1250–1259
DOI 10.1007/s10904-015-0234-1

The Novel Poly(azomethine-urethane): Synthesis, Morphological Properties and Application as a Fluorescent Probe for Detection of Zn^{2+} Ions

Musa Kamacı[1,2] · İsmet Kaya[1]

Received: 6 February 2015 / Accepted: 2 May 2015 / Published online: 7 May 2015

Abstract In this paper reports synthesis of a new kind of Schiff base-polyurethane containing azomethine linkage and uses of this poly(azomethine-urethane) as fluorescence probe for determination of transition metal ions in aqueous medium. The spectroscopic behavior of poly(azomethine-urethane) toward metal ions has been investigated by the fluorescence method and photoluminescence (PL) characteristics of compounds were investigated in different polarity solvents including MeOH, tetrahydrofurane (THF) and dimethylformamide (DMF). PL measurements showed that both Schiff base and polymer have higher emission intensity and Stoke's shift value ($\Delta\lambda_{ST}$) in THF solution than DMF and MeOH. The proposed sensor was found to show good selectivity to Zn^{2+} ion over other metal ions in THF/deionized water solution (1:2, v:v). Notably, the proposed sensor could clearly distinguish Zn^{2+} from Cd^{2+}. Detection limit of the proposed sensor was also determined as 3.06×10^{-4} mol L^{-1}.

Keywords Poly(azomethine-urethane) · Schiff base · Fluorescent sensor · Sensing zinc ion · Zn(II) sensor · Zinc

1 Introduction

Along with the various kinds of chemical sensors, fluorescent sensors have many advantages such as high sensitive, simple manipulation, facile visualization, low cost, ease of handling and real-time monitoring with fast response time due to photoluminescence (PL) measurements [1–3]. Because of these advantages, fluorescent sensors or probes for biologically active metal ions have been considerable interest in recent years and they are a lot of applications in the field of material, biological and environmental sciences [4, 5].

Among the various kinds of transition metal ions, zinc is the second most abundant transition metals in human body after iron [6]. Zn^{2+} plays a significant role in various physiological and pathological processes such as gene expression, enzyme regulation, neurotransmission, apoptosis regulation [7], DNA binding or recognition [8], neural signal transmission [9] and brain function [10]. Additionally, Zn^{2+} exists in various biological systems including pancreas, prostate, retina and brain [11, 12]. This metal ion is also known to have a role in neurological disorders, such as Alzheimer's disease, cerebral ischemia, epilepsy, amyotrophic lateral sclerosis (ALS), Parkinson's disease and hypoxia ischemia [13, 14]. On the other hand, excessive quantities of Zn^{2+} intake may lead to both acute and chronic toxicity, and excessive concentration of this metal ion may reduce the soil microbial activity resulting in phytotoxic effects [15, 16]. Moreover, zinc ion (Zn^{2+}) has similar coordination properties with cadmium ion (Cd^{2+}) and they are difficult to distinguish due to they are both in the IIB group elements of the periodic table [17]. Because of these properties, Zn^{2+} and Cd^{2+} ions often respond together with similar spectral changes. Therefore, there is a great importance to developing fluorescencent Zn^{2+}

✉ İsmet Kaya
kayaismet@hotmail.com

[1] Polymer Synthesis and Analysis Laboratory, Department of Chemistry, Faculty of Sciences and Arts, Çanakkale Onsekiz Mart University, 17020 Çanakkale, Turkey

[2] Department of Chemistry, Faculty of Sciences and Arts, Piri Reis University, Tuzla, 34940 Istanbul, Turkey

selective sensor or probe that distinguish Zn^{2+} from other transition metal ions especially Cd^{2+} in the biological system, material and environmental science.

In this paper, we have designed and prepared a Schiff base-polymeric fluorescent probe for detection of transition metal ions including Cd^{2+}, Co^{2+}, Cr^{3+} Cu^{2+}, Mn^{2+}, Ni^{2+}, Pb^{2+}, Zn^{2+} and Cr^{3+}. Polymeric probe was prepared in two steps. In the first step, Schiff base was synthesized by condensation reaction of 2,2′-dithio-dianiline with 4-(diethylamino)salicylaldehyde. In the second step, this preformed Schiff base was converted to polyurethane derivative by step-polymerization using toluene diisocyanate. As known, Schiff base or azomethine (–N=CH) ligand exhibits a strong affinity for transition metal ions due to nitrogen atom in the structure and they have special coordination ability with transition metal ions [18]. The prepared compounds were characterized by FT-IR, ^{1}H, ^{13}C-NMR and SEC techniques. Photophysical behaviors of Schiff base and its poly(azomethine-urethane) derivative were studied in different polarity solvents such as dimethylformamide (DMF), MeOH or tetrahydrofurane (THF), and in presence of different metal ions, focusing the attention on their emission properties using fluorescence spectroscopy. To the best of our knowledge, there are only a few paper in literature about poly(azomethine-urethane)-based fluorescent sensor or probe for determination of transition metal ion in aqueous solution.

2 Experimental

2.1 Materials

2,2′-Dithio-dianiline (TDA), 4-(diethylamino)salicylaldehyde (SAL), toluene diisocyanate (TDI), acetone, acetonitrile (MeCN), carbon tetrachloride (CCl_4), chloroform ($CHCl_3$), DMF, ethanol (EtOH), ethyl acetate, methanol (MeOH), *n*-hexane, THF, toluene, $Mn(CH_3COO)_2{\cdot}H_2O$ and $Pb(CH_3COO)_2{\cdot}3H_2O$ were supplied from Merck Chemical Co. (Germany), $Cd(CH_3COO)_2{\cdot}2H_2O$, $Co(CH_3COO)_2{\cdot}4H_2O$, $Cu(CH_3COO)_2{\cdot}H_2O$, $Ni(CH_3COO)_2{\cdot}4H_2O$ and $Zn(CH_3COO)_2{\cdot}2H_2O$ were from Fluka, $CrCl_3$ and $ZrCl_4$ were from Riedel–Dehaen, and all the reagents were used without further purification.

2.2 Synthesis of 6,6′-((1Z,1′Z)-((disulfanediylbis(2,1-phenylene))bis(azanylylidene)) bis(methanylylidene))bis(3-(diethylamino)phenol) (SPAMEP)

SPAMEP was prepared by the condensation of 2,2′-dithio-dianiline (TDA, 2.484 g, 1×10^{-2} mol) with 4-(diethylamino)salicylaldehyde (SAL, 3.865 g, 2×10^{-2} mol) in MeOH (30 mL) by stirring the mixture under reflux for 3 h, and then cooling at room temperature (Scheme 1). The Schiff base was washed with MeCN (2×50 mL) to remove the unreacted components and dried in a vacuum desiccator at 75 °C [19].

Yield: 88 %. ^{1}H-NMR (DMSO-d_6, δ_{pmp}): 10.06 (–O<u>H</u>), 8.78 (–imine (–N=C<u>H</u>)), 7.75, 7.54, 7.50, 7.43, 7.39, 6.41 and 6.13 (aromatic protons), 3.45 (–C<u>H</u>$_2$–CH$_3$) and 1.19 (–CH$_2$–C<u>H</u>$_3$). ^{13}C-NMR (DMSO-d_6, δ_{pmp}): 162.55 (–<u>C</u>–OH), 159.50 ((–imine (–N=<u>C</u>H)), 156.47, 153.80, 140.12, 136.44, 132.73, 128.84, 125.50, 117.60, 111.82, 109.35, 104.48 (aromatic carbons), 47.60 (–<u>C</u>H$_2$–CH$_3$) and 13.40 (–CH$_2$–<u>C</u>H$_3$).

2.3 Synthesis of (5-(diethylamino)-2-((Z)-((2-((Z)-(4-(diethylamino)-2-methoxybenzylidene) amino)cyclohexa-1,3-dien-1-yl)disulfanyl) phenyl)imino)methyl)phenyl (5-acetamido-2-methylphenyl)carbamate) (P-SPAMEP)

P-SPAMEP was prepared by the step polymerization reaction of the preformed Schiff base (1.197 g, 2×10^{-3} mol) in DMF/THF (1/3) mixture (60 mL) with TDI (0.348 g, 2×10^{-3} mol) in THF (30 mL) by stirring the mixture. Reaction was maintained for 6 h under argon atmosphere and, then mixture cooled at the room temperature and kept for 24 h (Scheme 1). P-SPAMEP was washed with MeOH (2×50 mL) and MeCN (2×50 mL) to remove the unreacted components and dried in a vacuum oven at 75 °C for 24 h [20].

Yield: 79 %. ^{1}H-NMR (DMSO-d_6, δ_{pmp}): 9.72 (urethane–N<u>H</u>) 8.93 (–imine (–N=C<u>H</u>)), 7.98, 7.68, 7.46, 7.39, 7.34, 7.30, 7.25, 7.21, 6.68 and 6.49 (aromatic protons) 3.48 (–C<u>H</u>$_2$–CH$_3$), 2.18 (–C<u>H</u>$_3$) and 1.24 (–CH$_2$–C<u>H</u>$_3$), ^{13}C-NMR (DMSO-d_6, δ_{pmp}): 168.84 (urethane–<u>C</u>=O), 160.26 (imine (–N=<u>C</u>H)), 157.65, 154.24, 151.82, 138.58, 136.43, 134.78, 132.85, 130.7, 129.13, 127.84, 126.95, 124.87, 118.33, 117.97, 114.58, 113.20, 111.72, 108.14 (aromatic carbons), 47.63 (–<u>C</u>H$_2$–CH$_3$), 18.16 (–<u>C</u>H$_3$), and 13.36 (–CH$_2$–<u>C</u>H$_3$), SEC: Mn: 21,600 g mol^{-1}, Mw: 39,800 g mol^{-1}, PDI:1.843.

2.4 Preparation of the Stock Solutions

A 1.00×10^{-3} M solution of P-SPAMEP (4.01×10^{-2} g, 5.00×10^{-5} mol) was prepared in 50 mL DMF, MeOH or THF, respectively. Solutions of Cd^{2+}, Co^{2+}, Cu^{2+}, Mn^{2+}, Ni^{2+}, Pb^{2+} and Zn^{2+} were prepared from their acetate salts while solutions of Cr^{3+} and Zr^{2+} prepared from their chloride salts. Concentrations of these solutions were adjusted as 1.00×10^{-1} M in deionized water. These prepared stock solutions were also used in all measurements.

Scheme 1 Synthesis scheme of SPAMEP and P-SPAMEP

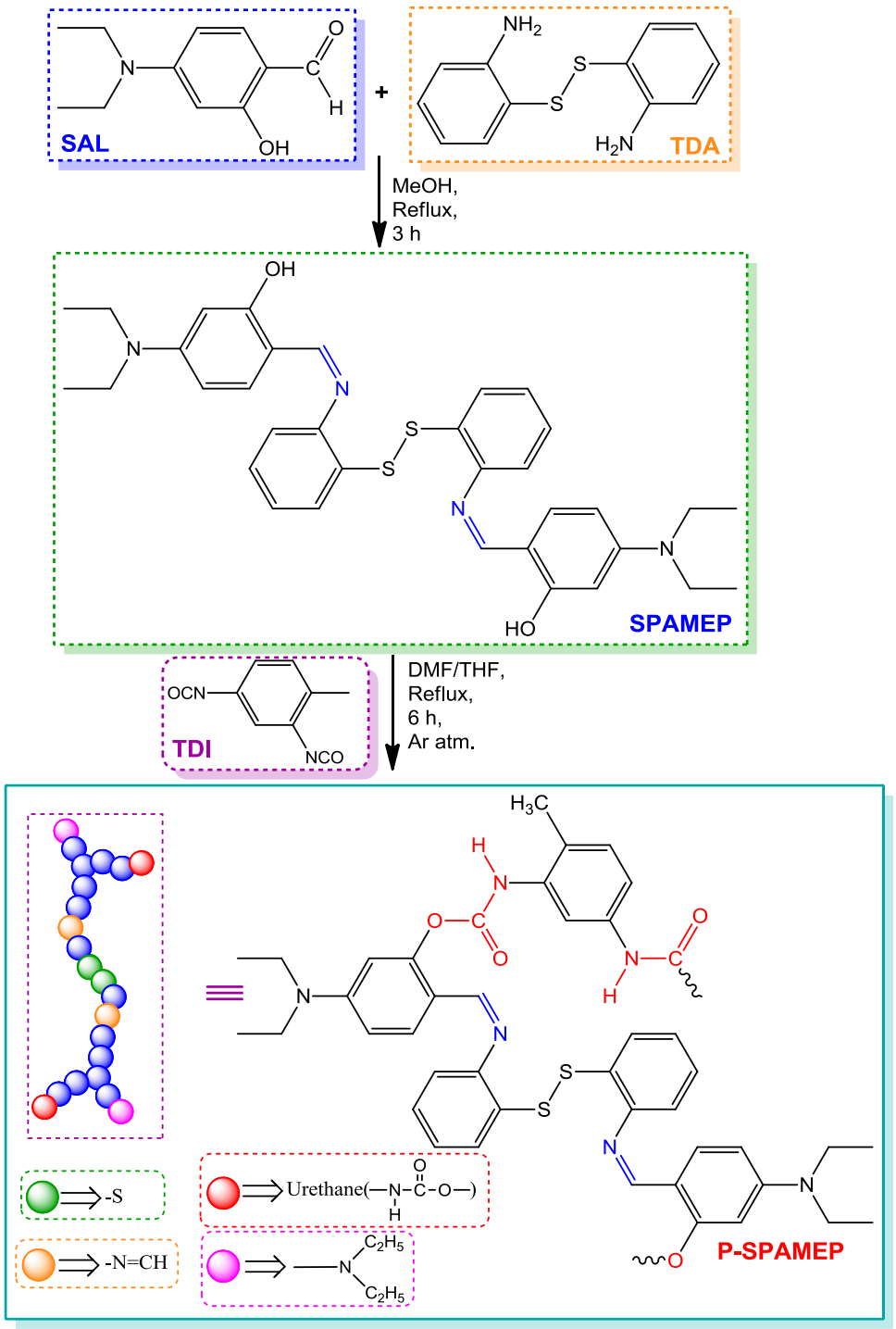

2.5 Characterization Techniques

The infrared spectra were obtained by Perkin Elmer FT-IR Spectrum one using the universal ATR sampling accessory (4000–550 cm^{-1}). ^{1}H and ^{13}C-NMR spectra (Bruker AC FT-NMR spectrometer operating at 400 and 100.6 MHz, respectively) were recorded in deuterated DMSO-d_6 at 25 °C. Tetramethylsilane (TMS) was used as internal standard. The number-average molecular weights of poly(azomethine-urethane) were determined by size exclusion chromatography (SEC) technique of Shimadzu Co. For SEC investigations, an SGX (100 Å and 7 nm diameter loading material) 3.3 mm i.d. × 300 mm columns was used; eluent: DMF (0.4 ml min^{-1}), polystyrene standards

were used. A refractive index detector (RID) was used to analyze the products at 25 °C.

2.6 Fluorescence Measurements

A Shimadzu RF-5301PC spectrofluorophotometer was used for fluorescence measurements. PL measurements of SPAMEP and P-SPAMEP were carried out in MeOH, THF and DMF solutions. Emission spectra of these compounds were obtained MeOH, THF and DMF with the concentration of 1×10^{-3} M SPAMEP and P-SPAMEP due to determine the optimal emission and excitation wavelengths in each solvent. The effects of transition metal ions on quenching-growing of the emission spectra were investigated in 1:2 (v:v) THF/deionized water solutions each of which containing 1×10^{-3} M of P-SPAMEP and 1×10^{-1} M metal ion. The changes of fluorescence intensities depending on the concentration of Zn^{2+} ions were determined using a series of different concentrated metal solutions in THF/deionized water mixtures (1:2, v:v). Excitation and emission slit width was adjusted as 5 nm in the mentioned experiments. Another series of Zn^{2+} containing P-SPAMEP solutions were prepared to determine the detection limit. For this purpose several solutions with different concentrated Zn^{2+} in the range 1.000×10^{-3} to 3.125×10^{-5} M were used. In detection limit experiments excitation slit width was adjusted as 10 nm while the emission slit was kept as 5 nm. This slit change made the intensity differences more detectable due to the increasing separation of emission peaks from each other. Fluorescence quantum yield (Φ_F) is calculated by comparative methods using rhodamine 6G solution in ethanol as in the literature [21].

2.7 Morphological Properties

Atomic force microscopy (AFM) topography and 3D images of P-SPAMEP were recorded using WITec Alpha 300A AC mode (cantilever 42 N/m 285 kHz) AFM instrument. The measurements were carried out at room temperature. The system is covered with an acoustic chamber to prevent electromagnetic impacts, which may disturb the measurements.

3 Results and Discussion

3.1 Solubility and Characterization

The prepared SPAMEP and P-SPAMEP are red and dark-red colored powder compounds, respectively. According to the solubility tests results, P-SPAMEP is soluble in THF and DMF partly soluble in MeOH and EtOH whereas it is insoluble in *n*-hexane, benzene, toluene, acetone, MeCN, $CHCl_3$, CCl_4 and ethyl acetate.

The chemical structures of SPAMEP and P-SPAMEP were verified by FT-IR, NMR and SEC analyses. FT-IR spectra of SAL, TDA, SPAMEP, TDI and P-SPAMEP were shown in Fig. 1. According to FT-IR spectra of SAL, hydroxyl (–OH), aldehyde (–CHO) and aliphatic –CH stretch vibrations are observed at 3288 and 1620 cm^{-1}, respectively. Amine ($–NH_2$) and –C–S stretch vibrations of TDA are observed at 3376 and 745 cm^{-1}, respectively [22]. After the condensation reaction of these two compounds stretch vibrations (aldehyde and amine) disappear and the new stretch vibration appears at 1635 cm^{-1} indicating imine (–N=CH) stretch vibration. Also, hydroxyl (–OH), aliphatic –CH and –C–S stretch vibrations of SPAMEP are observed at 3298, 2972 and 753 cm^{-1}, respectively. As can be seen in Fig. 1, characteristic isocyanate stretch vibrations (–N=C and –C=O) of TDI are observed at 1615 and 2230 cm^{-1}, respectively [23]. After the step-polymerization reaction of SPAMEP and TDI, isocyanate stretch vibrations of TDI and hydroxyl (–OH)

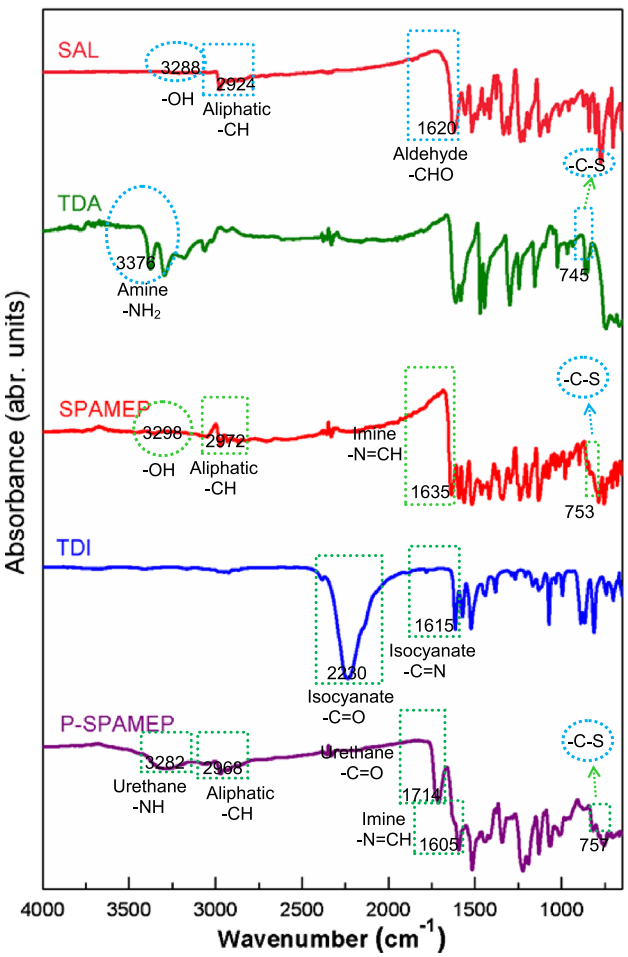

Fig. 1 FT-IR spectra of starting materials, SPAMEP and P-SPAMEP

stretch vibration of SPAMEP disappear due to urethane formation. According to FT-IR spectrum of P-SPAMEP, urethane –NH and –C=O, imine (–N=CH), –C–S and aliphatic –CH stretch vibrations are observed at 3282, 1714, 1605, 2968 and 757 cm^{-1}, respectively. These spectral data clearly confirm the formation of proposed SPAMEP and P-SPAMEP in Scheme 1. Additionally, NMR spectral data of SPAMEP and P-SPAMEP were given in experimental section.

3.2 PL Characteristics of SPAMEP and P-SPAMEP

To investigate of the solvent effect on SPAMEP and P-SPAMEP, the excitation and emission spectra of these compounds (1.00×10^{-3} M) were recorded in different polarity solvents such as MeOH, THF or DMF using PL spectrophotometer (Fig. 2). The fluorescence spectral data of SPAMEP and P-SPAMEP were also summarized in Table 1. Emission intensities of SPAMEP and P-SPAMEP are determined as 21 and 70 in MeOH, 37 and 122 in THF and 16 and 8 in DMF, respectively. Stoke's shift values of SPAMEP and P-SPAMEP are also found as 71 and 75 nm in MeOH, 80 and 102 nm in THF, 60 and 62 nm in DMF, respectively. These obtained results shown that, SPAMEP and P-SPAMEP have higher emission intensity and Stoke shift value in THF solution than the other solvents. This can be probably polarity of solvents (polarity order of solvents: DMF > MeOH > THF) [24, 25]. Furthermore, Stoke's shift is very important parameter for fluorescence sensor or probe due to the higher Stoke's shift value supplies very low background signals and resultantly allows the usage of the material in construction of a fluorescence sensor [26]. Also, the quantum yield (Φ_F) of P-SPAMEP-Zn^{2+} solution and in the absence of Zn^{2+} ions was found to be 4.6 and <0.04 %, respectively.

3.3 Selective of P-SPAMEP Fluorescence Response by Zn(II)

1.00×10^{-1} M solutions of Cd^{3+}, Co^{2+}, Cr^{2+}, Cu^{2+}, Mn^{2+}, Ni^{2+}, Pb^{2+}, Zn^{2+} and Zr^{4+} were used to investigate the metal ion selection of P-SPAMEP, as shown in Fig. 3. In these selectivity studies, polyurethane concentration adjusted as 1.00×10^{-3} M due to minimize the PL intensity of metal-free polymer solution in working range. The obtained results were also summarized in Table 2. It can be seen that the emission peak of Cd^{2+}, Zr^{4+}, Ni^{2+} and Zn^{2+} is increased at 487 nm while this peak of Pb^{2+},

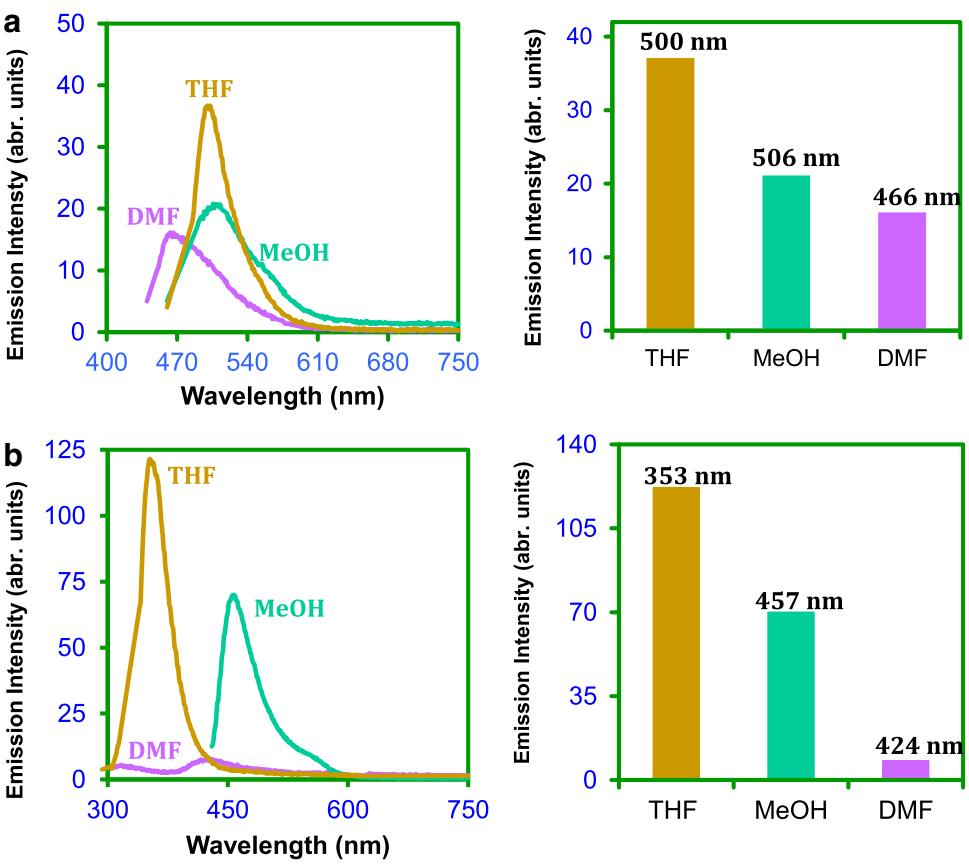

Fig. 2 Emission spectra of SPAMEP (**a**) and P-SPAMEP (**b**) in different polarity solvents

Table 1 PL measurement data of SPAMEP and P-SPAMEP

Solvent	$\lambda_{Ex.}$ (nm)[a]	$\lambda_{Em.}$ (nm)[b]	$\lambda_{max\ (Ex.)}$ (nm)[c]	$\lambda_{max\ (Em.)}$ (nm)[d]	$I^{e}_{Ex.}$	$I^{f}_{Em.}$	$\Delta\lambda^{g}_{ST}$
MeOH[h]	408	452	435	506	18	21	71
THF[h]	395	444	420	500	32	37	80
DMF[h]	383	429	406	466	13	16	60
MeOH[i]	368	407	382	457	66	70	75
THF[i]	238	326	251	353	115	122	102
DMF[i]	302	342	361	423	6	8	62

[a] Excitation wavelength for emission

[b] Emission wavelength for excitation

[c] Maximum excitation wavelength

[d] Maximum emission wavelength

[e] Maximum excitation intensity

[f] Maximum emission intensity

[g] Stokes shift value : $\left[\lambda_{max(Em.)} - \lambda_{max(Ex.)}\right]$

[h] Compound: SPAMEP

[i] Compound: P-SPAMEP

Mn^{2+}, Co^{2+}, Cr^{3+} and Cu^{2+} is decreased at the same wavelength. According to Table 2, the emission intensities of Cu^{2+}, Cr^{3+}, Co^{2+}, Mn^{2+}, Pb^{2+}, Cd^{2+}, Ni^{2+}, Zr^{4+} and Zn^{2+} are found as 55, 78, 112, 126, 134, 150, 165, 213 and 966 at 487 nm respectively. According to these results, Zn^{2+} has about 4.5 and 17.5 times more emission intensity than Zr^{4+} and Cu^{2+}, respectively. These results indicatates that P-SPAMEP could be used as very selective Zn^{2+} sensor in aqueous solution.

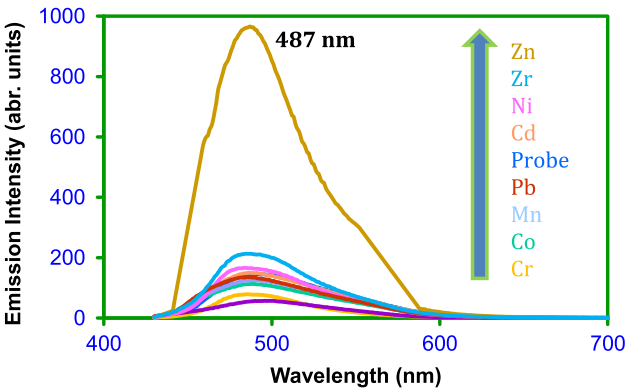

Fig. 3 PL spectra of P-SPAMEP (1.00×10^{-3} M) with presence of 1.00×10^{-1} M metal ions (conditions: $\lambda_{Ex} = 238$ nm, $\lambda_{Em} = 326$ nm, slit: $\lambda_{Ex} = 5$ nm, $\lambda_{Em} = 5$ nm)

3.4 Concentration Effect of Zn(II) on P-SPAMEP

The fluorescence property of P-SPAMEP and its responses of Zn^{2+} ion concentration were investigated in THF/deionized water (1:2, v:v) at 487 nm (Fig. 4a). As can be seen in Fig. 4a, with the decreases of Zn^{2+} ion concentration the emission intensity continuously decreased. Also, 3D images of emission intensity changes of Zn^{2+} ion concentration was shown in Fig. 4b.

To calculate regression equations and coefficients, relative emission intensities $(I - I_o/I_o)$ at 487 nm were obtained from Fig. 4. Then, these intensities were plotters vs. Zn^{2+} ion concentration in the range 1.000×10^{-3} to 3.125×10^{-5} M, as shown in Fig. 5. Also, the obtained equations were given in Eqs. 1 and 2.

$$\frac{I - I_o}{I_o} = 5158.8\left[Zn^{2+}\right] + 0.7848 \quad (R_1 = 0.9415) \qquad (1)$$

$$\frac{I - I_o}{I_o} = 10401\left[Zn^{2+}\right] - 0.8207 \quad (R_2 = 0.9996) \qquad (2)$$

where I is the emission intensity of tested metal ion at 487 nm and I_0 is the emission intensity of metal free polyurethane solution. According to these results, a good linearity relationship is obtained with regression coefficient $R_1 = 0.9415$ and $R_2 = 0.9996$. These calculated regression equations and coefficients could be assumed that the novel fluorescent poly(azomethine-urethane) had potential

Table 2 Fluorescence measurement data of P-SPAMEP in the presence of transition metal ions

Metal Ions	Cu(II)	Cr(III)	Co(II)	Mn(II)	Pb(II)	Cd(II)	Ni(II)	Zr(IV)	Zn(II)
I_{em} (487 nm)[a]	55	78	112	126	134	150	165	213	966

[a] Emission intensity at 487 nm

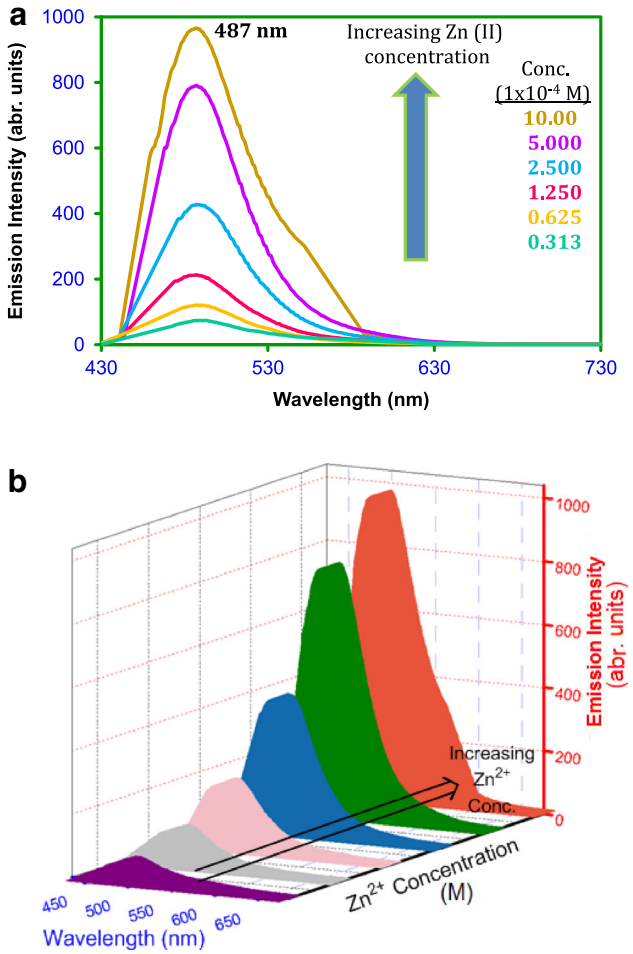

Fig. 4 Emission intensity changes of P-SPAMEP upon addition of different amounts of Zn^{2+} in THF/de-ionized water (1:2) (conditions: $\lambda_{Ex} = 238$ nm, $\lambda_{Em} = 326$ nm, Slit: $\lambda_{Ex} = 5$ nm, $\lambda_{Em} = 5$ nm) (**a**) and 3D images of increasing Zn^{2+} concentration (**b**)

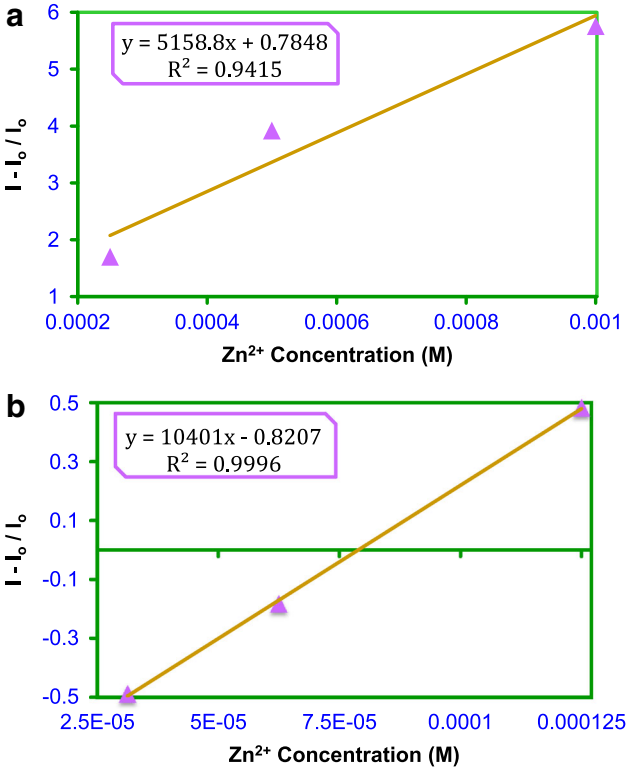

Fig. 5 A plot of the relationship between Zn^{2+} concentration and relative emission intensities

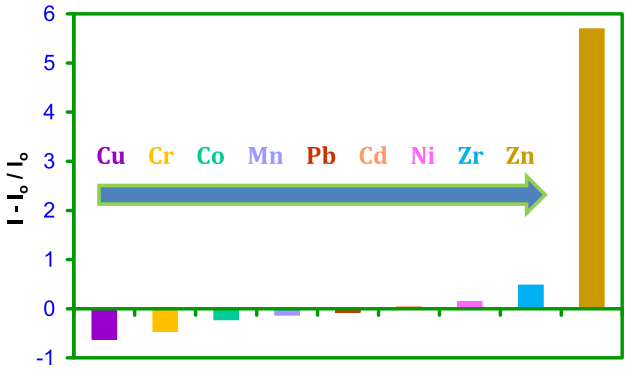

Fig. 6 Interference effect on P-SPAMEP in the presence of different metal ions (1×10^{-1} M) at 487 nm

prospects as a selective detector of Zn^{2+} ion in aqueous environment.

The detection limit of sensor is another important parameter in sensor applications. The detection limit of Zn^{2+} sensor was calculated as in the literature [27] and the detection limit of sensor was calculated as 3.06×10^{-4} mol L^{-1}.

3.5 Interference Study

To investigate interference and anti-interference effect of the other transition metal ions, interference study of the proposed sensor was carried out using 1×10^{-1} M metal ion and 1×10^{-3} M stock polyurethane solution at 487 nm (Fig. 6). The obtained results shown that P-SPAMEP and Zn^{2+} solution mixture have the highest relative intensity (5.69). Also, this mixture have about 12, 38 and 142 times more relative intensity than Zr^{4+} (0.48), Ni^{2+} (0.15) and Zr^{4+} (0.04), respectively.

On the other hand, according to the electronic configuration of these transitional metal ions, Cd^{2+} and Zn^{2+} ions have similar electronic configuration in last orbits. Both Cd^{2+} and Zn^{2+} ions have d^{10} electronic structure in last orbits. Due to this property, Zn^{2+} fluorescent probe can also respond to Cd^{2+} [28]. In this study, the proposed Zn^{2+} fluorescent probe was not responded to Cd^{2+} and it could clearly distinguish Zn^{2+} from Cd^{2+}.

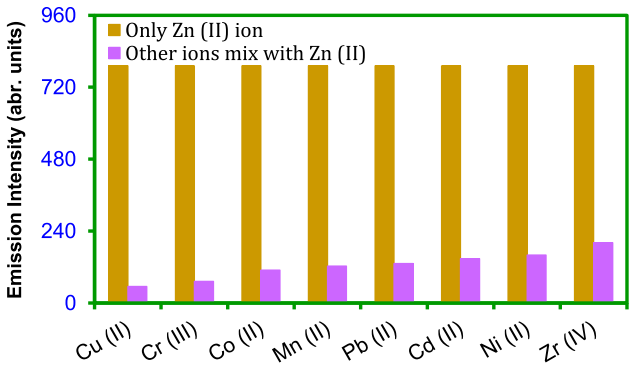

Fig. 7 Quenching ion effect on the proposed fluorescent sensor

3.6 Quenching Ion Effect

Quenching ion effect on the proposed fluorescent sensor were investigated using 1×10^{-3} M P-SPAMEP, 1×10^{-1} M Zn^{2+} in THF/deionized water (2:1, v:v) and 1 mg metal ion such as Cd^{2+}, Co^{2+}, Cr^{3+}, Cu^{2+}, Mn^{2+}, Ni^{2+}, Pb^{2+} or Zr^{4+} as shown in Fig. 7. As can be seen in Fig. 7, the presence of some transitional metal ions such as Cd^{2+}, Co^{2+}, Cr^{3+}, Cu^{2+}, Mn^{2+}, Ni^{2+}, Pb^{2+} or Zr^{4+} caused only slight changes in the emission spectra of the proposed sensor.

3.7 Binding Model and Responsive Mechanism

To determine binding model between P-SPAMEP and Zn^{2+}, molecular orbital charge density and charge of atom or groups in P-SPAMEP was calculated using Huckel calculation method [27]. Figure 8a shows the molecular orbital charge density of P-SPAMEP. As can be seen in Scheme 1, –S–S, imine (–N=CH), urethane (–NH), (–C=O) and (–O–) groups or atoms composed a conjugated chromophore moiety in the proposed sensor. According to Fig. 8a, imine nitrogens (–N=CH) and –S–S groups have higher charge density than urethane group. This indicates that the possible complexation could be mainly carried out between these groups.

The calculated charge of atom or groups in structure of poly(azomethine-urethane) is shown in Fig. 8b. As can be seen in Fig. 8b, charge of sulfur atom in –S–S bond, nitrogen atom in imine group (–N=CH), nitrogen (–NH), oxygen (–O) and carbon atoms (–C=O) in urethane bonding are calculated as −0.1015, −0.629, −0.547, −0.2325 and −0.57, respectively. According to these results, imine nitrogens have quite higher negative charges than the other heteroatoms.

The possible structure of Zn^{2+} with P-SPAMEP is given in Fig. 8c. As known, polymeric Schiff base contain one or

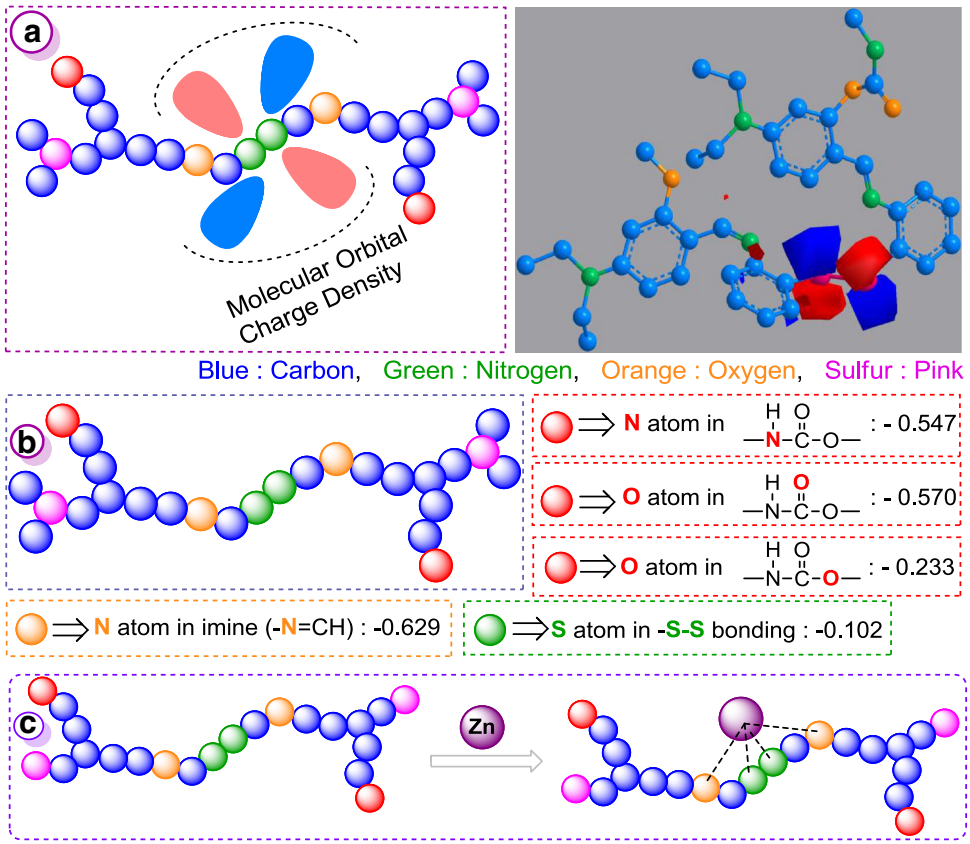

Fig. 8 The molecular charge density (**a**), calculated charges of atoms or groups in poly(azomethine-urethane)s (**b**) and possible structure of the proposed sensor (**c**)

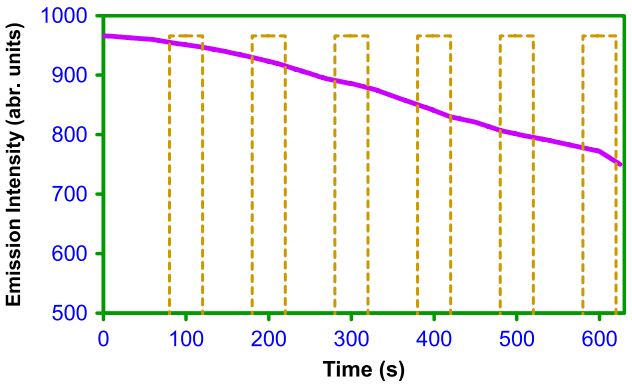

Fig. 9 The time resolved photoluminescence spectrum of poly (azomethine-urethane) (1×10^{-3} M) and Zn^{2+} ion (1×10^{-1} M) complex in THF

more imine (–N=CH) linkages in the structures and they readily form stable complexes with most of the metal ions [29]. According to these explanations, calculated molecular orbital charge diagram and charges of atoms or groups in the structure of poly(azmethine-urethane)s, the possible complexation could be mainly carried out with the imine nitrogens and –S–S bond.

3.8 The Time-Resolved Curve

The time resolved PL spectrum of P-SPAMEP (1×10^{-3} M) and Zn^{2+} ion (1×10^{-1} M) complex in THF/deionized water solution (1:2, v:v) is shown in Fig. 9 and results are also summarized in Table 3. As can be seen in Fig. 9 and Table 3, the fluorescence lifetime data of the proposed sensor were found as 0.62, 1.97, 3.73, 6.10, 8.28, 10.97, 14.08, 16.46, 18.22 and 20.08 % for 60, 120, 180, 240, 300, 360, 420, 480, 540 and 600 s, respectively. These obtained results shown that P-SPAMEP and Zn^{2+} complex is quite stable.

3.9 Morphological Properties

Morphological properties of poly(azomethine-urethane)s were investigeted by using AFM, as shown in Fig. 10. This technique was used in order to evaluate the evolution of topography and the phase roughness of P-SPAMEP. According to AFM images of the proposed polymeric probe, the surface of this compound seems to be rough and dense with non-uniform dispersion.

4 Conclusion

A novel Schiff base-polyurethane containing azomethine linkage was successfully synthesized and designed as fluorescent sensor for detection of transition metal ions in aqueous solutions. The spectroscopic behavior of poly (azomethine-urethane) was investigated using fluorescence measurements in different polarity solvents (DMF, MeOH and THF). Fluorescence measurements shown that the proposed probe have higher emission intensity and Stoke's shift

Table 3 The time-resolved data of P-SPAMEP and Zn^{2+} ion complex in THF/deionized water

Time (s)	0	60	120	180	240	300	360	420	480	540	600
Wavelength (nm)	966	960	947	930	907	886	860	830	807	790	772
Degradation (%)	–	0.62	1.97	3.73	6.10	8.28	10.97	14.08	16.46	18.22	20.08

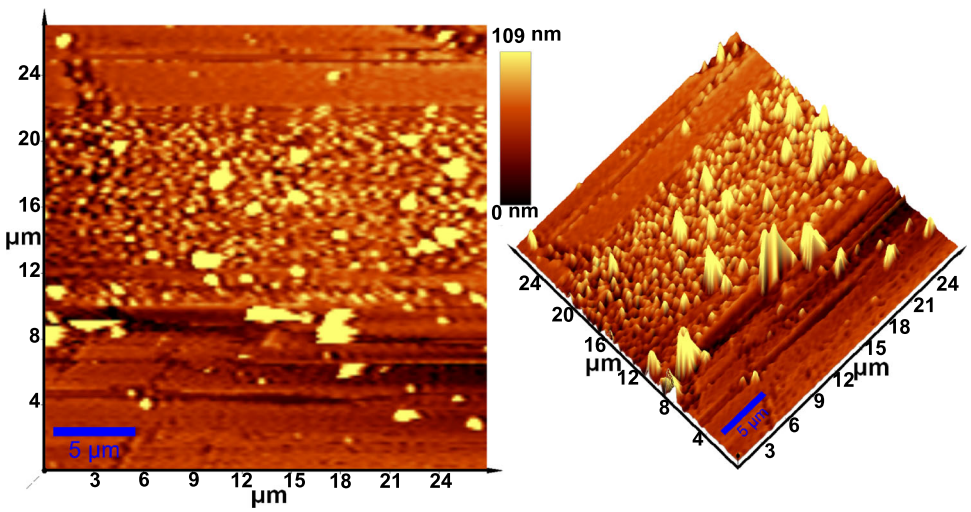

Fig. 10 AFM image of P-SPAMEP

value ($\Delta\lambda_{ST}$) in THF solution than the other solvents. The proposed sensor was found to show good selectivity to Zn^{2+} ion over other metal ions in THF/de-ionized water solution (1:2, v:v). Notably, the proposed sensor could clearly distinguish Zn^{2+} from Cd^{2+} and possible interference and quenching effect of the other tested transition metal ions were found too low. Detection limit of the proposed sensor was also determined as 3.06×10^{-4} mol L^{-1}.

References

1. D. Zhang, J.R. Cochrane, A. Martinez, G. Gao, RSC Adv. **4**, 29735–29749 (2014)
2. T. Hong, H. Song, X. Li, W. Zhang, Y. Xie, RSC Adv. **4**, 6133–6140 (2014)
3. S. Anbu, R. Ravishankaran, M.F.C. Guedes da Silva, A.A. Karande, A.J.L. Pombeiro, Inorg. Chem. **53**, 6655–6664 (2014)
4. K. Tayade, S.K. Sahoo, B. Bondhopadhyay, V.K. Bhardwaj, N. Singh, A. Basu, R. Bendre, A. Kuwar, Biosens. Bioelectron. **61**, 429–433 (2014)
5. L. Wang, W. Qin, W. Liu, Anal. Methods **6**, 1167–1173 (2014)
6. H.M. Liu, P. Venkatesan, S.P. Wu, Sensor. Actuat. B-Chem. **203**, 719–725 (2014)
7. L. Wang, W. Qin, W. Liu, Inorg. Chem. Commun. **13**, 1122–1125 (2010)
8. J. Sun, T. Yu, H. Yu, M. Sun, H. Li, Z. Zhang, H. Jiang, S. Wang, Anal. Methods **6**, 6768–6773 (2014)
9. E.L. Que, D.W. Domaille, C.J. Chang, Chem. Rev. **108**, 1517–1549 (2008)
10. E. Mocchegiani, C. Bertoni-Freddari, F. Marcellini, M. Malavolta, Prog. Neurobiol. **75**, 367–390 (2005)
11. A. Takeda, Biometals **14**, 343–351 (2001)
12. C.J. Frederickson, L.J. Giblin III, B. Rengarajan, R. Masalha, C.J. Frederickson, Y. Zeng, E.V. Lopez, J.Y. Koh, U. Chorin, L. Besser, M. Hershfinkel, Y. Li, R.B. Thompson, A. Krezer, J. Neurosci. Methods **154**, 19–29 (2006)
13. N. Roy, H.A.R. Pramanik, P.C. Paul, S.T. Singh, J. Fluoresc. **24**, 1099–1106 (2014)
14. L. Li, F. Liu, H.W. Li, Spectrochim. Acta A-M. **79**, 1688–1692 (2011)
15. M. Iniya, D. Jeyanthi, K. Krishnaveni, A. Mahesh, D. Chellappa, Spectrochim. Acta A-M. **120**, 40–46 (2014)
16. A. Voegelin, S. Pfister, A.C. Scheinost, M.A. Marcus, R. Kretzschmar, Changes in Zinc Speciation in Field Soil after Contamination with Zinc Oxide. Environ. Sci. Technol. **39**, 6616–6623 (2005)
17. J.T. Hou, B.Y. Liu, K. Li, K.K. Yu, M.B. Wu, X.Q. Yu, Talanta **116**, 434–440 (2013)
18. L. Salmon, P. Thuéry, E. Rivière, M. Ephritikhine, Inorg. Chem. **45**, 83–93 (2006)
19. M. Kamacı, I. Kaya, J. Macromol. Sci. A **51**, 805–819 (2014)
20. M. Kamacı, I. Kaya, J. Inorg. Organomet. Polym. **24**, 803–818 (2014)
21. C. Ben-nan, H. Qin, H. Yan, J. Chun-man, Z. Qi, Chem. Res. Chin. Univ. **29**(3), 419–423 (2013)
22. V. Somerset, J. Leaner, R. Mason, E. Iwuoha, A. Morrin, Electrochim. Acta **55**, 4240–4246 (2010)
23. I. Kaya, M. Kamacı, Prog. Org. Coat. **74**, 204–214 (2012)
24. D.A. Yushchenko, V.V. Shvadchak, M.D. Bilokin, A.S. Klymchenko, G. Duportail, Y. Mely, V.G. Pivovarenko, Photochem. Photobiol. Sci **5**, 1038–1044 (2006)
25. X. Yang, H. Lyu, K. Chen, X. Zhu, S. Zhang, J. Chen, Bio. Resour. **9**(3), 5219–5233 (2014)
26. I. Kaya, M. Yıldırım, M. Kamacı, Synth. Met. **161**, 2036–2040 (2011)
27. I. Kaya, M. Kamacı, J. Fluoresc. **23**, 115–121 (2013)
28. N. Saleh, A.M.M. Rawashdeh, Y.A. Yousef, Y.A. Al-Soud, Spectrochim. Acta A-M. **68**, 728–733 (2007)
29. N.S. Abdel-Kader, R.R. Mohamed, J. Therm. Anal. Calorim. **114**, 603–611 (2013)